Phase closure retrieval in an infrared-to-visible upconversion interferometer for high resolution astronomical imaging

Damien Ceus,[1] **Alessandro Tonello,**[1] **Ludovic Grossard,**[1] **Laurent Delage,**[1] **François Reynaud,**[1,*] **Harald Herrmann,**[2] **and Wolfgang Sohler**[2]

[1]*XLIM Département Photonique, Université de Limoges, UMR CNRS 6172, 123 Av. A. Thomas, 87060 LIMOGES CEDEX, France*

[2]*Universität Paderborn, Angewandte Physik, Warburger Str. 100 - 33098 PADERBORN, Germany*

**francois.reynaud@xlim.fr*

Abstract: This paper demonstrates the use of a nonlinear upconversion process to observe an infrared source through a telescope array detecting the interferometric signal in the visible domain. We experimentally demonstrate the possibility to retrieve information on the phase of the object spectrum of an infrared source by using a three-arm upconversion interferometer. We focus our study on the acquisition of phase information of the complex visibility by means of the phase closure technique. In our experimental demonstration, a laboratory binary star with an adjustable photometric ratio is used as a test source. A real time comparison between a standard three-arm interferometer and our new concept using upconversion by sum-frequency generation demonstrates the preservation of phase information which is essential for image reconstruction.

OCIS codes: (350.1260) Astronomical optics; (120.3180) Interferometry; (110.1650) Coherence imaging; (070.0070) Fourier optics and signal processing; (060.2310) Fiber optics; (190.4223) Nonlinear wave mixing; (160.3730) Lithium niobate.

References and links

1. M. Wittkowski, P. Kervella, R. Arsenault, F. Paresce, T. Beckert and G. Weigelt, "VLTI/VINCI observations of the nucleus of NGC 1068 using the adaptive optics system MACAO," Astron. Astrophys. **3,** L39–L42 (2004).
2. P. Wizinowich, D. S. Acton, C. Shelton, P. Stomski, J. Gathright, K. Ho, W. Lupton, K. Tsubota, O. Lai, C. Max, J. Brase, J. An, K. Avicola, S. Olivier, D. Gavel, B. Macintosh, A. Ghez, and J. Larkin, "First light adaptive optics images from the Keck II telescope: a new era of high angular resolution imagery," Publ. Astron. Soc. Pac. **112,** 315–319 (2000).
3. M. I. Ye, H. K. Aroji, H. A. Ndo, N. K. Aifu, K. Kodaira, K. Aoki, W. Aoki, Y. C. Hikada, Y. D. Oi, N. E. Bizuka, B. E. Lms, G. F. Ujihara, H. F. Urusawa, T. F. Use, W. G. Aessler, S. Arasawa, Y. H. Ayano, M. H. Ayashi, S. H. Ayashi, S. I. Chikawa, M. I. Manishi, C. I. Shida, Y. K. Amata, T. K. Anzama, N. K. Ashikawa, K. K. Awabata, N. Kobayashi, Y. Komiyama, G. Kosugi, T. K. Urakami, M. L. Etawsky, Y. M. Ikami, A. M. Iyashita, S. M. Iyazaki, Y. M. Izumoto, J. M. Orino, K. M. Otohara, K. M. Urakawa, M. Nakagiri, K. Nakamura, H. Nakaya, K. Nariai, T. N. Ishimura, K. N. Oguchi, T. N. Oguchi, J. N. Oumaru, R. O. Gasawara, N. O. Hshima, Y. O. Hyama, K. O. Kita, K. O. Mata, M. Otsubo, S. Oya, R. P. Otter, Y. S. Aito, T. S. Asaki, S. S. Ato, D. S. Carla, K. S. Chubert, K. S. Ekiguchi, M. S. Ekiguchi, I. S. Helton, C. S. Impson, H. S. Uto, A. Tajitsu, H. Takami, T. Takata, N. Takato, R. Tamae, M. Tamura, W. Tanaka, H. T. Erada, Y. Torii, F. U. Raguchi, T. U. Suda, M. W. Eber, T. W. Inegar, M.

#143071 - $15.00 USD Received 22 Feb 2011; revised 24 Mar 2011; accepted 24 Mar 2011; published 18 Apr 2011

Yagi, T. Yamada, T. Yamashita, Y. Yamashita, N. Yasuda, M. Yoshida, and M. Y. Utani, "Current Performance and On-Going Improvements of the 8.2m Subaru Telescope," Astron. Soc. Jap. **56,** 381–397 (2004).
4. P. R. Lawson, *Selected Papers on Long Baseline Stellar Interferometry* (SPIE Milestones Series, 1976).
5. R. G. Petrov, F. Malbet, G. Weigelt, P. Antonelli, U. Beckmann, Y. Bresson, A. Chelli, M. Dugu, G. Duvert, S. Gennari, L. Glck, P. Kern, S. Lagarde, E. Le Coarer, F. Lisi, F. Millour, K. Perraut, P. Puget, F. Rantakyr, S. Robbe-Dubois, A. Roussel, P. Salinari, E. Tatulli, G. Zins, M. Accardo, B. Acke, K. Agabi, E. Altariba, B. Arezki, E. Aristidi, C. Baffa, J. Behrend, T. Blcker, S. Bonhomme, S. Busoni, F. Cassaing, J.-M. Clausse, J. Colin, C. Connot, A. Delboulb, A. Domiciano de Souza, T. Driebe, P. Feautrier, D. Ferruzzi, T. Forveille, E. Fossat, R. Foy, D. Fraix-Burnet, A. Gallardo, E. Giani, C. Gil, A. Glentzlin, M. Heiden, M. Heininger, O. Hernandez Utrera, K.-H. Hofmann, D. Kamm, M. Kiekebusch, S. Kraus, D. Le Contel, J.-M. Le Contel, T. Lesourd, B. Lopez, M. Lopez, Y. Magnard, A. Marconi, G. Mars, G. Martinot-Lagarde, P. Mathias, P. Mge, J.-L. Monin, D. Mouillet, D. Mourard, E. Nussbaum, K. Ohnaka, J. Pacheco, C. Perrier, Y. Rabbia, S. Rebattu, F. Reynaud, A. Richichi, A. Robini, M. Sacchettini, D. Schertl, M. Schller, W. Solscheid, A. Spang, P. Stee, P. Stefanini, M. Tallon, I. Tallon-Bosc, D. Tasso, L. Testi, F. Vakili, O. von der Lhe, J.-C. Valtier, M. Vannier, and N. Ventura, "AMBER, the near-infrared spectro-interferometric three-telescope VLTI instrument," Astron. Astrophys. **12,** 1–12 (2007).
6. H. A. McAlister, T. A. ten Brummelaar, D. R. Gies, W. Huang, W. G. Bagnuolo, Jr., M. A. Shure, J. Sturmann, L. Sturmann, N. H. Turner, S. F. Taylor, D. H. Berger, E. K. Baines, E. Grundstrom, and C. Ogden, "First Results from the CHARA Array. I. An Interferometric and Spectroscopic Study of the Fast Rotator α Leonis (Regulus)," Astrophys. J. **628,** 439–452 (2005).
7. D. Leisawitz, C. Baker, A. Barger, D. Benford, A. Blain, R. Boyle, R. Broderick, J. Budinoff, J. Carpenter, R. Caverly, P. Chen, S. Cooley, C. Cottingham, J. Crooke, D. DiPietro, M. DiPirro, M. Femiano, A. Ferrer, J. Fischer, J. P. Gardner, L. Hallock, K. Harris, K. Hartman, M. Harwit, L. Hillenbrand, T. Hyde, D. Jones, J. Kellogg, A. Kogut, M. Kuchner, B. Lawson, J. Lecha, M. Lecha, A. Mainzer, J. Mannion, A. Martino, P. Mason, J. Mather, G. McDonald, R. Mills, L. Mundy, S. Ollendorf, J. Pellicciotti, D. Quinn, K. Rhee, S. Rinehart, T. Sauerwine, R. Silverberg, T. Smith, G. Stacey, H. P. Stahl, J. Staguhn, S. Tompkins, J. Tveekrem, S. Wall, and M. Wilson, "The space infrared interferometric telescope (SPIRIT): high-resolution imaging and spectroscopy in the far-infrared," Adv. Space Res. **40,** 689–703 (2007).
8. R. C. Jennision, "A phase sensitive interferometer technique for the measurement of the fourier transforms of spatial brithness distributions of small angular extent," R. Astron. Soc. **3,** 276–284 (1958).
9. G. Huss, F. Reynaud, and L. Delage, "An all guided three-arm interferometer for stellar interferometry," Opt. Commun. **196,** 55–62 (2001).
10. O. Absil, J.-B. Le Bouquin, J. Lebreton, J.-C Auguereau, M. Benisty, G. Chauvin, C. Hanot, A. Mérand, and G. Montagnier, "Deep near-infrared interferometric search for low-mass companions around β Pictoris," Astron. Astrophys. **520,** 1–7 (2010).
11. G. T. Van Belle, "Closure Phase Signatures of Planet Transit Events," Publ. Astron. Soc. Pac. **120,** 617–624 (2008).
12. L. Delage and F. Reynaud, "Analysis and control of polarization effects on phase closure and image acquisition in a fiber-linked three-telescope stellar interferometer," J. Opt. A: Pure Appl. Opt. **2,** 1–7 (2000).
13. V. Coudé Du Foresto, "Single-mode guided optics and astronomical interferometry," C. R. Acad. Sci, Ser. II **325,** 177–180 (1997).
14. E. Tatulli, N. Blind, J. P. Berger, A. Chelli, and F. Malbet, "Estimating the phase in ground-based interferometry: performance comparison between single-mode and multimode schemes," Astron. Astrophys. **524,** 1–22 (2010).
15. S. Brustlein, L. Del Rio, A. Tonello, L. Delage, F. Reynaud, H. Herrmann, and W. Sohler, "Laboratory Demonstration of an Infrared-to-Visible Up-Conversion Interferometer for Spatial Coherence Analysis," Phys. Rev. Lett. **100,** 153903 (2008).
16. M. Born and E. Wolf, *Principles of Optics* (Pergamon Press, 1980).
17. S. Olivier, L. Delage, F. Reynaud, V. Collomb, M. Trouillon, J. Grelin, I. Schanen, V. Minier, J. Broquin, C. Ruilier, and B. Leone, "MAFL experiment: development of photonic devices for a space-based multiaperture fiber-linked interferometer," Appl. Opt. **46,** 834–844 (2007).
18. M. A. Albota and F. N. C. Wong, "Efficient single-photon counting at 1.55 μm by means of frequency upconversion," Opt. Lett. **29,** 1449–1451 (2004).
19. C. Langrock, E. Diamanti, R. V. Roussev, Y. Yamamoto, and M. M. Fejer, "Highly efficient single-photon detection at communication wavelengths by use of upconversion in reverse-proton-exchanged periodically poled LiNbO3 waveguides," Opt. Lett. **30,** 1725–1727 (2005).
20. L. Delage, F. Reynaud, and A. Lannes, "Laboratory imaging stellar interferometer with fiber links," Appl. Opt. **39,** 6406–6420 (2000).
21. R. T. Thew, H. Zbinden, and N. Gisin, "Tunable upconversion photon detector," Appl. Phys. Lett. **93,** 1–3 (2008).

#143071 - $15.00 USD Received 22 Feb 2011; revised 24 Mar 2011; accepted 24 Mar 2011; published 18 Apr 2011

1. Introduction

Currently, the biggest monolithic or segmented optical telescopes such as the Very Large Telescope [1], the Keck [2] or Subaru telescopes [3], have diameters in the range of 10 m. This size limitation leads to an angular resolution in the range of 0.1 μrad for a 1 μm wavelength. To overcome this problem, it is possible to use the aperture synthesis technique, which was firstly demonstrated by Michelson [4]. For this purpose, the optical fields collected by two telescopes T_iT_j, spaced by a distance called baseline, are combined together. This two-telescope array works as a two-arm interferometer, and its highest angular resolution is related to the longest baseline. These diluted apertures are used to reach nano-radian angular resolution in ground based observatories such as VLTI [5] and CHARA [6] or in space missions [7]. These kinds of optical instruments are designed to analyze the spatial angular intensity distribution of an astronomical object. At the output of the interferometer, the detected signal, hereafter called the interferometric signal, is a fringe pattern modulated by the theoretical complex fringe visibility $V_{th} = C_{th}\exp(j\varphi_{th})$. For a pair of telescopes, C_{th} is the fringe contrast and φ_{th} the phase, both related to the object spectrum. As discussed below in this letter, the Zernike Van Cittert theorem gives a relation between the visibility V_{th} and the object spatial angular intensity distribution $O(\vec{\Omega})$, with $\vec{\Omega}$ the angular separation of the object under test. Figure 1 gives an example of C_{th} and φ_{th} plotted as a function of the normalized baseline. Note that for these two non-symmetric objects, spectra have the same modulus but different phases. Therefore, the ability to measure the phase of V_{th} remains mandatory for non-symmetric image reconstruction. Unfortunately, atmospheric turbulence and/or instrument instabilities (particularly in space mission) induce random phase shifts on the visibility function. Consequently, a direct measurement of φ_{th} is impossible. To overcome this limitation, Jennison proposed the use of the phase closure technique [8]. The phase closure term is theoretically unaffected by the atmospheric turbulences or by the instrument instabilities, and allows for example: image reconstruction [9], the detection of close faint companions in astronomy [10] or the signature of planet transit events [11]. The phase closure technique can be achieved only with a three (or more) arm interferometer. In this paper, we report for the first time to our knowledge, the observation of an infrared source by a sum-frequency conversion interferometer, using the Jennison's phase closure technique. In the following, this interferometer will be called upconversion interferometer. In our upconversion interferometer, the infrared light of the object under test, collected by each T_i telescope, is converted from infrared to visible wavelength. This way, the V_{th} complex visibility is acquired in the visible spectral domain. This experimental test has been achieved with a in-laboratory proof of principle experiment. This type of high angular resolution imaging instrument has to provide reliable contrasts and phase closure measurements. For this purpose, we took care to comply with the polarization [12] and spatial filtering [13, 14] requirements related to spatial coherence analysis. In a first step, we have developed our upconversion interferometer using telecommunication components to check that V_{th} is faithfully transfered from infrared to visible wavelength domain. In a previous work, the C_{ij} contrasts had been retrieved successfully in a two-arm upconversion interferometer [15]. The core of this paper describes the acquisition of the phase closure using our three-arm upconversion interferometer.

#143071 - $15.00 USD Received 22 Feb 2011; revised 24 Mar 2011; accepted 24 Mar 2011; published 18 Apr 2011

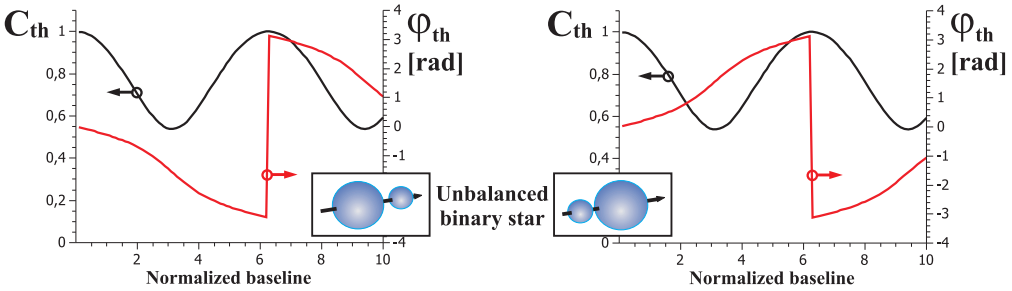

Fig. 1. Two different configurations of a non-symmetric object. The contrast and the phase of the object spectrum are plotted as a function of the normalized baseline between two telescopes. Without atmospheric turbulences, this phase is not corrupted and can be measured.

2. Description of the Jennison's phase closure technique

Figure 2 shows the principle of a one-dimension telescope array able to provide high angular resolution images for optical astronomy. The object under test is an unbalanced binary star with a spatial angular intensity distribution $O(\vec{\Omega})$, where $\vec{\Omega}$ is the angular separation. In our experimental setup, the binary star and the telescope array are along the same axis, so Ω_0 is the projection of $\vec{\Omega}$ on the axis of the telescope. In the Fig. 2 configuration, the baseline T_1T_2 (i.e the distance between T_1 and T_2) is fixed and equal to b. The distance T_2T_3 can be set to nb with n an integer.

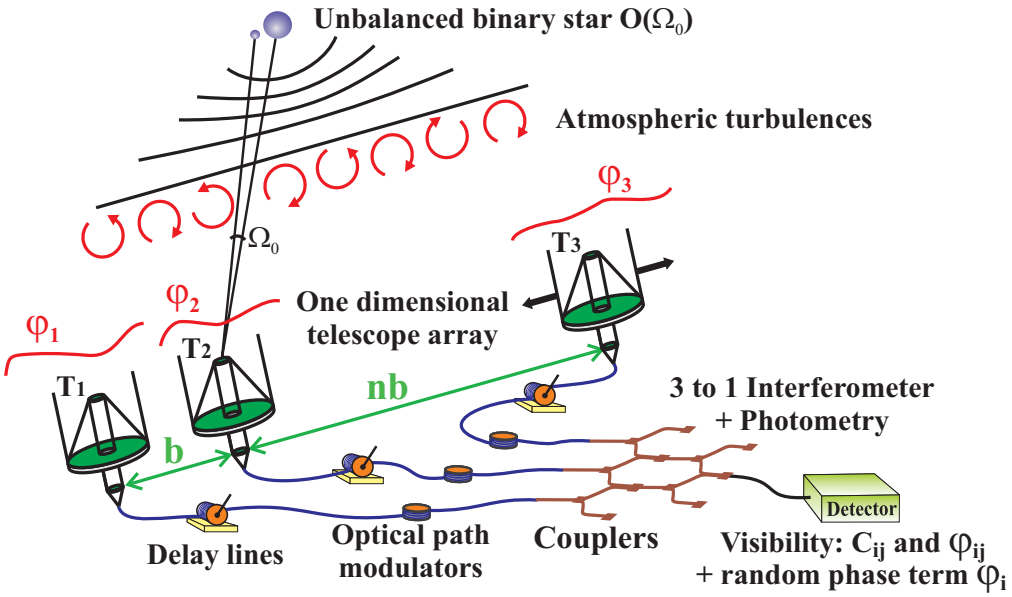

Fig. 2. Overview of a one-dimension telescope interferometer dedicated to high resolution imaging. $O(\Omega_0)$: spatial angular intensity distribution, Ω_0: angular separation. T_i is the i_{th} telescope. T_3 can be relocated in different positions equal to nb with n an integer and b the baseline between T_1T_2. Output data: fringe contrasts C_{ij} and object spectrum phases φ_{ij} related to a pair of telescopes T_iT_j corrupted by the turbulences phases φ_i at T_i and φ_j at T_j.

#143071 - $15.00 USD Received 22 Feb 2011; revised 24 Mar 2011; accepted 24 Mar 2011; published 18 Apr 2011

As seen previously, the complex visibility is equal to:

$$V_{th}(nb) = C_{th}\exp(j\varphi_{th}) \quad (1)$$

The Zernike Van Cittert theorem gives the relation between the theoretical complex visibility $V_{th}(nb)$ and the classical spatial angular intensity distribution $O(\Omega)$, see [16] for more details:

$$V_{th}(nb) = \frac{1}{I}\int_{object} O(\Omega)\exp(j2\pi nb\Omega/\lambda_{IR})d\Omega \quad (2)$$

where λ_{IR} is the mean wavelength of the analyzed radiation and I the total intensity emitted by the object. Equation (2) shows that the theoretical fringe visibility is equal to the Fourier Transform of the spatial angular intensity distribution:

$$V_{th}(nb) = (1/I)\tilde{O}(N) \quad (3)$$

with $\tilde{O}$ the object spectrum and $N = nb/\lambda_{IR}$ the spatial frequency. As shown on Fig. 2, two random phases φ_i and φ_j, related to the atmospheric turbulence, perturb the measurement of φ_{th}, the argument of $V_{th}(nb)$. Consequently, the experimental phase is shifted by $\varphi_i - \varphi_j$ preventing the φ_{ij} measurement:

$$V_{ij} = C_{ij}\exp[j(\varphi_i - \varphi_j + \varphi_{ij})] \quad (4)$$

Hence, each pair of the telescope array cannot provide any exploitable information on φ_{ij}. Thanks to Jennison's proposal, the phase closure technique allows to get a phase information directly related to the object spectrum phase. Let us describe this method.

In presence of atmospheric disturbances, the experimental complex visibility V_{ij} is given by Eq. (4). The phase closure ϕ is the linear combination of the arguments of the three experimental complex visibilities V_{12}, V_{23} and V_{31} related to the pairs of telescopes T_1T_2, T_2T_3 and T_3T_1 respectively:

$$\begin{aligned}\phi &= (\varphi_1 - \varphi_2 + \varphi_{12}) + (\varphi_2 - \varphi_3 + \varphi_{23}) + (\varphi_3 - \varphi_1 + \varphi_{31}) \\ &= \varphi_{12} + \varphi_{23} + \varphi_{31} \end{aligned} \quad (5)$$

The phase closure information is free of atmospheric disturbances.

The following part is dedicated to the description of an upconversion interferometer and how the phase closure technique was implemented.

3. Test of a laboratory high angular resolution upconversion interferometer

In this proof-of-principle experiment, the frequency upconversion took place in each arm of the upconversion interferometer. All the optical devices used in our test bench are polarization maintaining components and spatially single-mode. The wavelength conversion of a 1541 *nm* laboratory star to 630 *nm* was achieved in a Periodically Poled Lithium Niobate (PPLN) waveguide pumped by a 1064 *nm* YAG laser.

As seen previously, the phase closure technique requires at least, a three arm interferometer, so a third interferometric arm was added to our previous test bench. In order to demonstrate that the phase closure information can be transferred from the infrared to the visible spectral domain, we designed and implemented the three telescope interferometers as shown in Fig. 3. The experimental setup can be split up into four main subsystems:

#143071 - $15.00 USD Received 22 Feb 2011; revised 24 Mar 2011; accepted 24 Mar 2011; published 18 Apr 2011

a) The stars simulator: in our experimental configuration, the test-object is a binary star.

b) The telescopes array: three telescopes in a one-dimension linear configuration.

c) The infrared interferometer: classical interferometer in the infrared region used as a reference.

d) The upconversion interferometer: our new instrument under test.

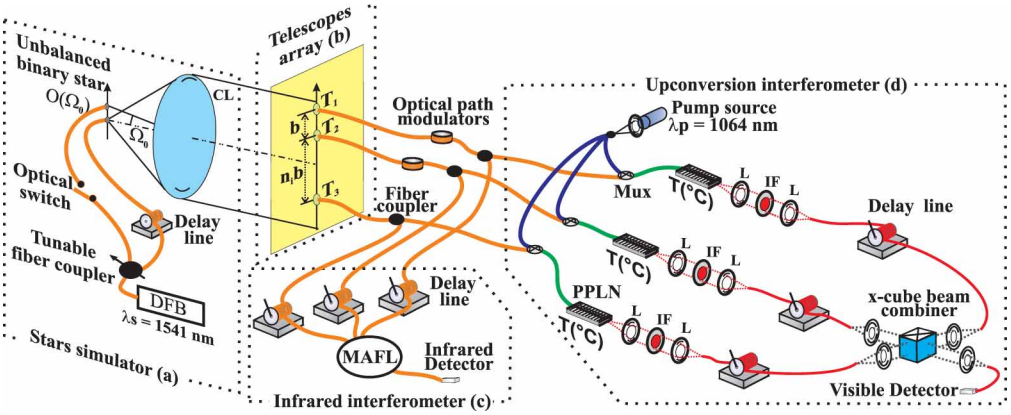

Fig. 3. Experimental setup of the upconversion test bench. DFB: Distributed Feed Back laser at 1541 *nm*, CL: Collimating Lens, *nb* the baseline between a pair of telescopes T_iT_j with *n* an integer, Mux: allows the combination of the signal at 1541 *nm* and 1064 *nm*, PPLN: Periodically Pooled Niobate Lithium, MAFL: Multi-Aperture Fibre Linked Interferometer, T($^\circ$C): temperature controller, IF: Interference Filter at $\lambda = 630\ nm \pm 20\ nm$, L: Lens. The delay lines are used for precision optical path length control in the infrared and visible interferometers.

For our proof of principle experiment, we used telecommunication wavelength sources and components for practical and cost reasons. Nonetheless, these experimental results can be transposed to other wavelength domains. In our experiment, the object to be imaged was an unbalanced laboratory binary star. For this purpose, a 1 to 2 fibre coupler, with an adjustable photometric ratio called μ, allowed to route the optical light emitted by a distributed feed back laser (DFB)($\lambda_{IR} = 1541\ nm$). The two fibre outputs acted as a point like sources spaced by 27.9 μm. The first coupler output was used directly as a point-like source. To ensure the spatial incoherence of this binary star, a 500 *m* fibred delay line was inserted in the second path, to induce an optical path difference longer than the 100 *m* coherence length of the DFB laser. The two fibre ends were placed in the focal plane of a collimating lens with a 1900 *mm* focal length and a 190 *mm* diameter. The resulting characteristics of our laboratory object corresponded to a binary star with an $\Omega_0 = 14.7\ \mu rad$ angular separation and an adjustable photometric ratio (μ). In our experimental configuration, the fluctuation of the air path between the star and the telescopes, and the small mechanical vibrations of the test bench acted as the atmospheric turbulence in a real telescope array.

In our experiment, assuming point-like sources, we can theoretically describe the angular intensity distribution of the object by:

$$O(\Omega) \quad = \quad \delta(\Omega - \Omega_0/2) + \mu\delta(\Omega + \Omega_0/2) \tag{6}$$

#143071 - $15.00 USD Received 22 Feb 2011; revised 24 Mar 2011; accepted 24 Mar 2011; published 18 Apr 2011

with δ denoting the Dirac delta distribution. The angular Fourier Transform of Eq. (6) gives the object spectrum $\tilde{O}$:

$$\tilde{O}(N) \quad = \quad \exp(-j\pi N\Omega_0) + \mu \exp(j\pi N\Omega_0) \tag{7}$$

The resulting phase φ_{ij} for a given spatial frequency N can be written as:

$$\arg[\tilde{O}(N)] \quad = \quad \arctan\left(\frac{\mu-1}{\mu+1}\tan(\pi N\Omega_0)\right) \tag{8}$$

The phase closure ϕ is derived from Eq. (8) according to Eq. (5). Note that ϕ varies as a function of the μ parameter driven by the adjustable photometric ratio of our fibre coupler. In the experimental setup, each telescope T_i was composed of an achromatic doublet ($f = 10$ *mm*). T_1T_2 was fixed and spaced by a $b = 16$ *mm* separation. T_3 can moved by steps equal to *nb*. The optical fields, collected at each telescope focus, were fed into single-mode optical fibres used as interferometric arms. Different optical path modulations had been applied to each interferometric arm in order to display the interferometric signal in the time domain. The Fourier Transform of this interferometric signal was composed of three frequencies related to the three pairs of telescopes. On each arm, a fibre coupler allowed to send 90% of the optical beam to our upconversion interferometer. The remaining 10% are routed to a classical infrared interferometer previously developed by our team for the Multi Aperture Fibre Linked Interferometer project [17] (bottom left Fig. 3). This infrared interferometer, used as a reference interferometer in our set up, had demonstrated its accuracy and reliability for the acquisition of the complex visibility of an infrared object.

In each arm of the upconversion interferometer, the infrared signal of the unbalanced binary star was mixed with a narrow-band pump source at 1064 *nm* and then injected in a PPLN waveguide. Each Ti-indiffused waveguide of 40 *mm* used had a 11.3 μm poling periodicity and was temperature stabilized at about 90^oC. This way, each signal was converted to a wavelength of about 630 *nm*. Notice that we did not focus our study on the conversion efficiency, that has been previously addressed for instance in [18, 19]. Each upconverted signal passed through an interference filter to block the residual pump radiation and then fed a single-mode fibre at 630 *nm*. In each arm, the upconverted optical fields were combined together with an X-cube (2002 patent 6363186 and [20]). This device had 4 inputs and 4 outputs. In our experimental configuration, it had been used as a symmetrical 3 to 1 coupler for the visible radiation mixing. The three upconverted interferometric arms were equalized. For this purpose the delay lines were tuned and the interferometric pattern was detected with a silicon avalanche photodiode. The raw data were analyzed to extract phase closure in the infrared and visible wavelengths at the same time.

4. Data acquisition processing and results

Figure 4 plots the phase terms as a function of time. As one can appreciate, the phase term $\varphi(T_iT_j)$, related to the pair of telescope T_iT_j, is not constant over the time but the phase closure remains constant over all the acquisition. The object was a point-like source and the data were recorded with the infrared interferometer.

For the acquisition of the phase closure, in a first step, we had to calibrate the infrared and the visible interferometer with a point-like source (one star was switched-off). The raw data coming from both interferometers were analyzed and calibrated. With a point-like star, the phase closure is theoretically equal to 0. The Fourier Transform applied to the interferometric data allowed to correct the experimental bias up to reach $\phi = 0$.

In a second stage, the secondary star was switched-on and the phase closures were recorded

#143071 - $15.00 USD Received 22 Feb 2011; revised 24 Mar 2011; accepted 24 Mar 2011; published 18 Apr 2011

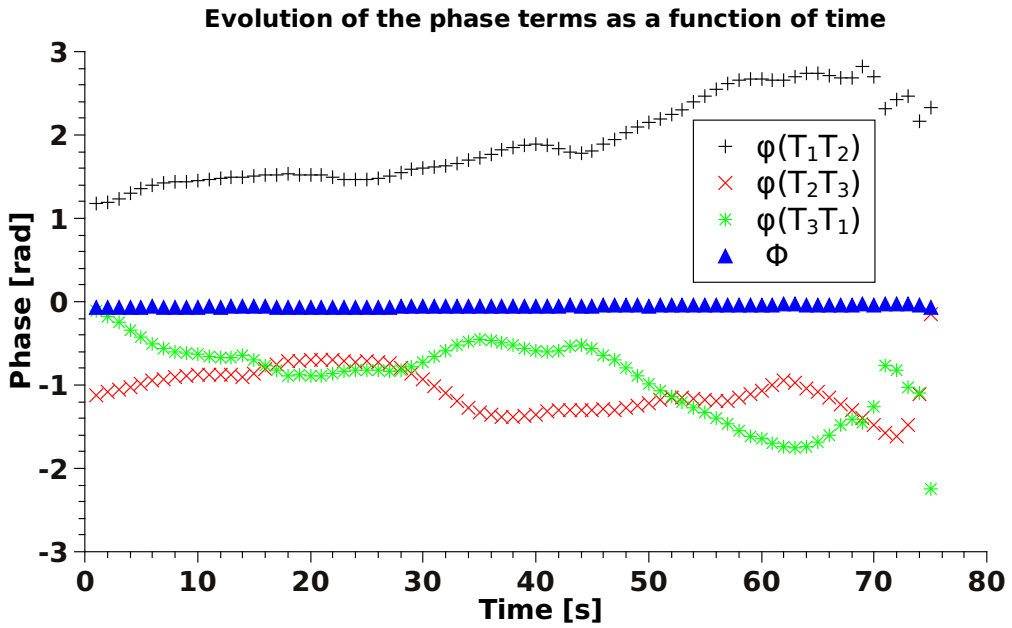

Fig. 4. The Phase terms of a point-like source are plotted for the three pairs of telescopes as a function of time. The phase closure term is the sum of the three phase terms.

for the infrared and the upconversion interferometers as a function of μ with a fixed baseline configuration of the telescope array. These two stages had been realized for two configurations of the telescope array (Fig. 5). In the first one, the distance between T_1T_2 was equal to b and T_2T_3 was equal to $2b$. In the second one, the distance between T_1T_2 was equal to b and T_2T_3 was equal to $3b$. These measurements, obtained with the visible interferometer, were compared with the theoretical data and with the infrared reference interferometer at the same time. Figure 5 shows an excellent accordance between theoretical predictions (green dashed curves) and the upconversion (blue crosses) and classical interferometric (red crosses) data. The theoretical curve is based on Eq. (8) and Eq. (5) written for a three-arm interferometer. Each experimental point results from the average over a set of 30 phase closure acquisitions. The error bars (not plotted) are on the order of 5 *mrad* and 10 *mrad* for the upconversion and the infrared interferometer respectively. These small uncertainties of the phase closure show the stability in time of our upconversion interferometer. The error bars related to the photometric ratio μ are around $\pm 3\%$ for each point.

5. Conclusion

This first proof-of-principle experiment clearly demonstrated that the phase closure can be transferred without any distortion into the visible spectral domain by using our upconversion interferometer. Being a key point for high resolution imaging, the phase closure acquisition after frequency conversion clearly demonstrates the reliability of our upconversion interferometer capabilities. We have developed our upconversion interferometer using single-mode and polarization maintaining components. To fit the astronomical observational constraints, we intend to operate our instrument with lower flux level (down to the photon-counting regime). We also have to work on broadband frequency conversion. Preliminary study on this point has already been realized [21] and we will have to adapt this technique in the high resolution

#143071 - $15.00 USD Received 22 Feb 2011; revised 24 Mar 2011; accepted 24 Mar 2011; published 18 Apr 2011

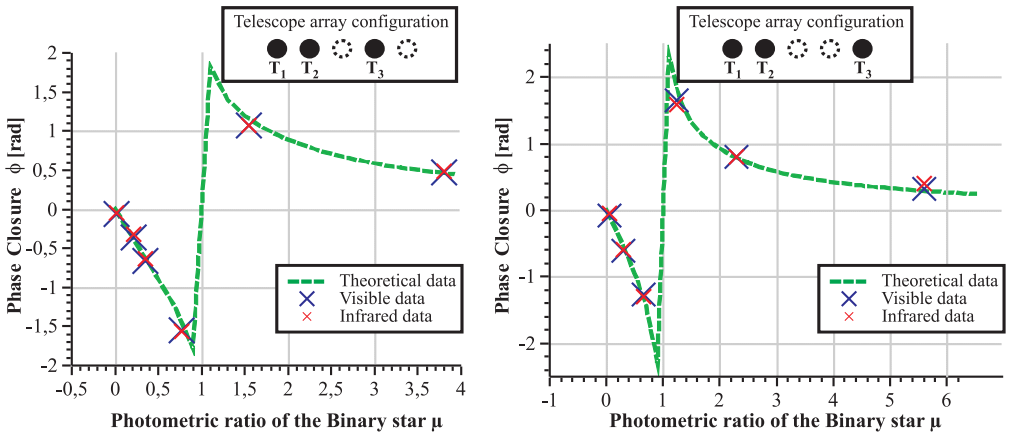

Fig. 5. Phase closure measurements as a function of the photometric ratio μ for two configurations of the telescope array. On the left (right) hand side *n=2(3)*. Red (blue) $\times$ plots the infrared (visible) data. Green dashed curves report the theoretical data.

interferometric context. Further, this new kind of interferometer will be applied to frequency conversion of broadband medium and/or far infrared spectra. In a more general way, the frequency conversion technique allows to benefit from mature optical components mainly used in optical telecommunications (waveguides, couplers, multiplexers…) and efficient low-noise detection schemes down to the single-photon counting level. Consequently, it could be possible to avoid lots of technical difficulties related to infrared optics (components transmission, thermal noises, thermal cooling, spatial filtering …). The frequency conversion technique could be used to have access to unexplored optical windows on ground observatories.

Acknowledgments

This work has been financially supported by the Centre National d'Etudes Spatiales (CNES) and by l'Institut National des Sciences de L'Univers (INSU). Our thanks go to A. Dexet for the development and his advices for all the specific mechanical components.

#143071 - $15.00 USD Received 22 Feb 2011; revised 24 Mar 2011; accepted 24 Mar 2011; published 18 Apr 2011